Outcome After Placement of Tantalum Porous Engineered Dental Implants in Fresh Extraction Sockets: A Canine Study

Jin Whan Lee, PhD[1]/Hai Bo Wen, PhD[2]/Suneel Battula, PhD[3]/Rama Akella, PhD[4]/
Michael Collins, MSE, MBA[5]/Georgios E. Romanos, DDS, PhD, Prof Dr Med Dent[6]

Purpose: *This study evaluated the stability and histologic proof of osseoincorporation of Trabecular Metal (TM) dental implants, which feature a tantalum-based porous midsection.* ***Materials and Methods:*** *A total of 48 TM implants (test group) and Tapered Screw-Vent implants (control group) were immediately placed bilaterally into mandibular extraction sockets in dogs. Resonance frequency analysis was performed at weeks 0, 2, 4, and 12 after implant placement. Histologic and histomorphometric evaluations of the implant interface were performed.* ***Results:*** *Changes in mean implant stability quotients (ISQ) revealed no statistical differences between the test and control groups. Histologic analysis showed bone ingrowth into the porous tantalum structure of all test group implants. Histomorphometric analysis revealed an increased percentage of bone-to-implant contact between 4 and 8 weeks in both test and control groups. The porous sections of the test group exhibited significantly more new bone inside the pores at week 12 in comparison to weeks 2 and 4. No correlation was observed between ISQ and histomorphometric parameters.* ***Conclusion:*** *In a canine immediate extraction socket model, both test and control implants demonstrated comparable implant stability and bone-to-implant contact. Bone ingrowth was evident within the tantalum porous section of the test implants during the early healing.* Int J Oral Maxillofac Implants 2015;30:134–142. doi: 10.11607/jomi.3692

Key words: *bone ingrowth, osseoincorporation, porous tantalum, trabecular metal dental implant*

Tantalum (Ta)-based, porous engineered implants have been scientifically and clinically documented for more than 15 years in orthopedic medicine.[1,2] In the biologic environment, Ta exhibits excellent compatibility and corrosion resistance.[3,4] Independent studies have documented the structural and mechanical properties of Ta porous biomaterial; its three-dimensional cellular structure is similar to cancellous bone, with a high coefficient of friction, high porosity (up to 80%), average pore size of 430 μm, and low modulus of elasticity (3 GPa).[5–7] These combined features uniquely differentiate the Ta porous biomaterial from other metallic biomaterials with lesser porosity, including sintered titanium bead surfaces, titanium plasma–sprayed surfaces, titanium fiber mesh, and titanium foam.[5,7–9]

In light of its success in orthopedic applications, the Ta porous biomaterial was applied to a multithreaded, tapered dental implant design. In addition to conventional bone-to-implant contact (osseointegration), a geometric network of interconnected pores is designed for bone ingrowth and propagation throughout the porous structure to augment anchorage of the implant.[10–12] The combination of bone-to-implant contact and bone ingrowth and propagation within the porous material has been termed *osseoincorporation*.[13] In a previous canine study, Ta porous dental implants placed in healed extraction sites demonstrated new bone formation within the Ta pores and stability similar to that of a conventional threaded implant.[14]

To shorten treatment time, an implant may be placed immediately into a fresh extraction socket. However, animal and human studies have reported

[1]Manager of Research, Zimmer Dental, Carlsbad, California, USA.
[2]Director of Research, Zimmer Dental, Carlsbad, California, USA.
[3]Research Engineer, Zimmer Dental, Carlsbad, California, USA.
[4]Staff Scientist, Zimmer Orthobiologics, Austin, Texas, USA.
[5]Vice President of Research & Development, General Manager of Zfx, Zimmer Dental, Carlsbad, California, USA.
[6]Professor, Stony Brook University, School of Dental Medicine, Stony Brook, New York, USA.

Correspondence to: Dr Georgios Romanos, Stony Brook University, School of Dental Medicine, 106 Rockland Hall, Stony Brook, NY 11794-8705. Fax: +631-632-8670. Email: georgios.romanos@stonybrook.edu

that extraction sockets experienced traumatic bone necrosis and significant ridge resorption.[15,16] As such, autogenous bone or bone graft substitute with or without a membrane has been recommended to support the preservation of alveolar ridge dimensions, especially in the presence of marginal defects after immediate placement of implants into fresh extraction sockets.[15,17,18]

The safety and effectiveness of the Ta porous dental implant in healed extraction sites have been confirmed. The objective of this study was to further evaluate the performance of the Ta porous dental implant in a clinically challenging situation—following placement in fresh extraction sockets in a canine model—with respect to implant stability and histologic proof of osseoincorporation. Clinically, it was hypothesized that the Trabecular Metal (TM) implant (Zimmer Dental) may be beneficial in preserving alveolar hard and soft tissues, as evidenced by adequate implant stability and distinctive osseoincorporation.

MATERIALS AND METHODS

Surgical Procedure

The study protocol was approved by the animal welfare committee at MPI Research Center. Six male hound dogs weighing 15.0 to 32.5 kg each were utilized in the study. A total of 48 implants of two different types were tested: 24 Tapered Screw-Vent MTX implants (Zimmer Dental) (control group) and 24 TM implants (Zimmer Dental) (test group). All implants were 4.1 mm in diameter and 13 mm in length. After the dogs were anesthetized, incisions were made bilaterally in the gingival sulci of the mandibular third and fourth premolars (P3 and P4) and the first and second molars (M1 and M2). Osteotomies were created in the sockets for the placement of implants (eight implants per dog). Subsequently, cover screws were secured to allow submerged healing. Puros cancellous particulate bone graft substitute (Zimmer Dental) and BioMend collagen membranes (Zimmer Dental) were used to fill any voids between the alveolar bone plates and the implants (Fig 1). The gingival flaps were sutured with 4-0 Vicryl resorbable surgical sutures (Ethicon). During the first week of healing, all dogs received antibiotics and analgesics. Two dogs each were examined after 2, 4, or 12 weeks of healing.

Implant Stability Measurements

The stability of each implant was assessed by resonance frequency analysis (RFA) (Osstell, Integration Diagnostics) according to Meredith et al,[19] with results reported in implant stability quotients (ISQs). The RFA was performed at implant placement (as baseline) and before necropsy after 2, 4, or 12 weeks of healing. Animals were sedated (acepromazine maleate 0.1 mg/kg subcutaneous or 0.25 mg/kg intramuscular and/or propofol 6.0 mg/kg intravenous) to facilitate measurements. The Smart Peg was attached (Osstell) and the ISQ measured using a sterile probe. Each implant was measured three times from four directions (mesial to distal, distal to mesial, lingual to buccal, and buccal to lingual).

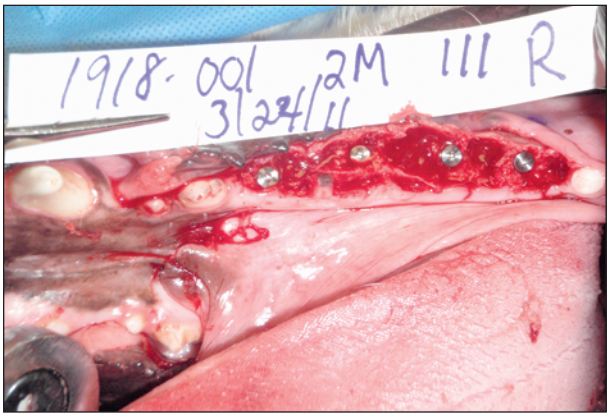

Fig 1 Placement of four implants in the left mandible.

Histologic and Histomorphometric Analysis

Euthanization by pentobarbital overdose was scheduled on weeks 2, 4, and 12 (two dogs at each time point). The mandibles were removed after death, and all implants were retrieved en bloc. Sutures were placed on the buccal side of the gingiva of each segment to indicate implant orientation postmortem. The specimens were immediately placed in 10% neutral buffered formalin for 48 hours. After fixation, the explanted tissue blocks were trimmed using a saw (Exakt 300 Band System, Exakt) to remove excessive soft tissue and dehydrated in an ascending series of concentrations of ethanol. Tissue blocks were then infiltrated with methacrylate-based resin (Technovit 7200, Heraeus Kulzer) according to the manufacturer's instructions. Undecalcified bone tissue blocks were cemented to the slides with an adhesive press (Exakt 401, Exakt) to maintain parallel surfaces.

The subsequent histologic experimental protocol was outlined by de Sanctis et al.[20] Briefly, a longitudinal section in the buccolingual direction at the midline was prepared from each tissue block with the Makro Trennsystem (Exakt Apparatebau). The sections were reduced to approximately 80 μm in thickness by grinding and polishing with a precision diamond saw (Isomet 2000, Buehler). All the sections were surface stained with Sanderson and Van Gieson (DHM) to distinguish between preexisting bone, mineralized new bone, and unmineralized osteoid. The stained final

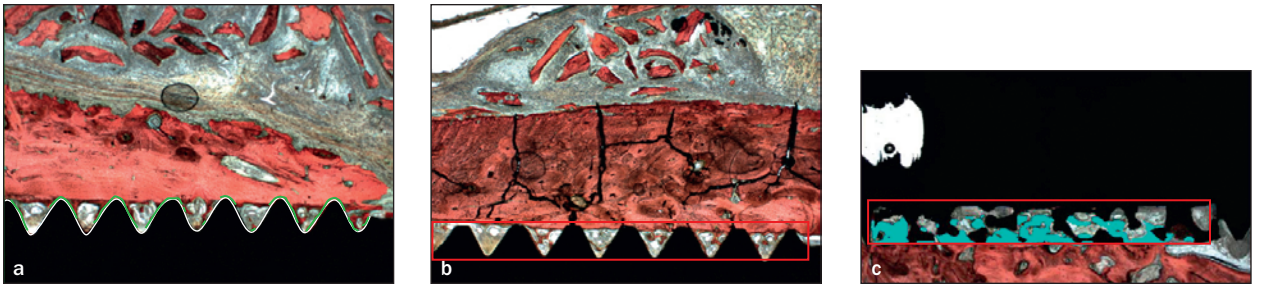

Fig 2 Histomorphometric measurements were performed based on the defined ROI to calculate the %BIC and % bone area fraction.

Table 1 Histomorphometric Parameters and Definitions

Measured parameter	Definition
Bone in contact, test group and control group: bone ongrowth	
Implant surface	Total implant surface perimeter in ROI
Bone in contact	Total length of bone surface in contact with implant in ROI
Osteoid in contact	Osteoid surface in contact with implant in ROI
Threaded portion, test group and control group: bone formation	
Region of interest	Entire ROI
Implant area	Implant area within the ROI
New bone formation area	New bone area within the ROI
Porous portion, test group only: bone ingrowth	
Region of interest	Implant area including pore space
Implant area	Implant area excluding pore space
New bone formation area	New bone area in implant area
Osteoid area	Osteoid area in implant area
Histomorphometric parameters	
%BIC	Bone in contact/implant surface × 100
%OIC	osteoid in contact/implant surface × 100
Available bone formation area	Region of interest area – implant area
%NBTA	New bone formation area/ available bone formation area × 100
Pore area	Region of interest area – implant area
%NBPA	New bone formation area/pore area × 100
%OPA	Osteoid formation area/pore area × 100

ROI = region of interest; %BIC = percent bone-implant contact; %OIC = % implant surface with osteoid contact; %NBTA = % available bone area with new bone formation: %NBPA = % occupied pore area with new bone formation; %OPA = % occupied pore area with osteoid formation.

slides, mounted on glass slides, were subjected to histopathologic and histomorphometric evaluation using a microscope (Olympus BH-2, Olympus Optical Co) and Bioquant Osteo II image analysis software (OsteoMetrics). The histologic features were evaluated at magnifications of ×2 to ×60.

Histopathologic assessment was performed to identify signs of bacterial infection, acute and chronic inflammation, and fibrosis. Inflammation was characterized by infiltration of inflammatory cells in the area surrounding the implant; acute inflammation was evidenced by the presence of neutrophils, and chronic inflammation was indicated by the infiltration of mononuclear inflammatory cells. A proliferation of fibroblasts and/or fibrocytes with deposition of collagen in the area surrounding the implant was characterized as fibrosis.

Table 1 defines the histomorphometric parameters, measures, and calculations used. The percentage of bone-to-implant contact (%BIC) for the control group was assessed within the range between the most coronal contact with bone and the apical end of the implant, as illustrated in Fig 2. The %BIC for the test group was measured as direct contact of bone with not only the coronal and apical threaded sections but also the marginal surfaces of the porous midsection (Fig 2a). The percent of osteoid in contact with the implant surface (%OIC) was defined as direct contact with osteoid within the same region of %BIC assessment.

The area of newly formed bone was measured for threaded and porous sections (Fig 2b). With regard to the control group, the region of interest (ROI) of newly formed bone found in threaded sections was first defined as the area encompassing the most coronal contact to the apical end of the implant. The new bone formation area was calculated by subtracting the area occupied by dental implant material from the ROI to assess the percentage of new bone in the threaded area (%NBTA). For the test group, the ROI of newly formed bone included the threaded areas of the implant at the coronal and apical parts (%NBTA). New bone formation area was then calculated by subtracting the area occupied by dental implant materials from the ROI. The new bone area in the porous midsection was measured separately for the test group to analyze bone ingrowth into the pores within the entire thickness of porous material on each side to assess the percentage of new bone formed in pore areas (%NBPA). The thickness of the porous Ta shell is 0.65 mm, and the depth of the thread pitch is 0.35 mm. The percent of osteoid

Table 2 ISQ Data Analysis

Time	Group	Mean	SD	*P* values between groups	*P* values, test group*	*P* values, control group
Week 0	Test	68	9	.6017	N/A	N/A
	Control	69	8			
Week 2	Test	67	10	.3103	.9641	.2091
	Control	64	11			
Week 4	Test	70	7	.4964	.4992	.5224
	Control	67	7			
Week 12	Test	71	4	.4919	.4193	.9369
	Control	69	10			

*Healing time vs baseline.

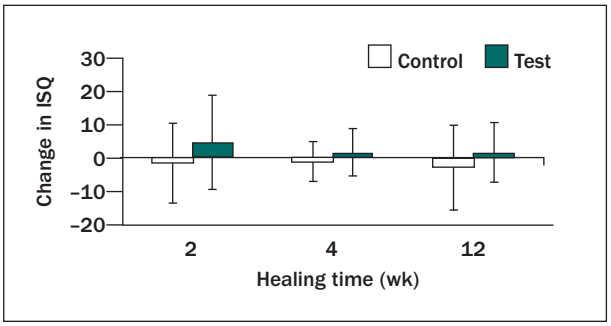

Fig 3 Changes in ISQs from baseline over the healing period. Comparisons were made between baseline (week 0) stability values and those measured in weeks 2, 4, and 12 in the control and test groups.

found in the pore area (%OPA) was also further measured within the same region of %NBPA assessment.

Statistical Analysis

With SAS software (version 9.2, SAS Institute), three-factor analysis of variance was used to compare the effects of implant type and healing time with the results of ISQ and histomorphometric data, followed by a post hoc Tukey test. Differences were considered significant at $P < .05$. Correlations between ISQs and histomorphometric data were calculated using the Pearson test, in which the 2-, 4-, and 12-week values were used to observe correlations between ISQs and histomorphometric values. Forty-eight pairs of values were applicable for correlation of ISQ, %BIC, and %NBTA, and 24 pairs of values were available for correlation of ISQs and %NBPA.

RESULTS

No implants failed during or after the surgery, so no implants were removed prior to the scheduled necropsy. With regard to immediate placement of implants into extraction sockets, the bone graft substitute and collagen membrane were applied to follow a principle similar to that reported in other experimental studies.[21,22] All grafted materials were well integrated, with no adverse reactions or biologic complications at the healing sites. The particulate grafts were observed in the crestal bone region during early healing and became more scattered because of resorption and/or remodeling during healing. Occasionally, encapsulation of particulates by connective tissue was observed, as was seen in a previous report.[23]

Implant Stability Measures

Mean ISQs at implant placement were 68 ± 9 for the test group and 69 ± 8 for the control group. The two groups showed no significant difference in ISQ at the time of placement ($P = .6017$). Mean ISQs for the test group were 67 ± 10, 70 ± 7, and 71 ± 4, and corresponding values of the control group were 64 ± 11, 67 ± 7, and 69 ± 10 after 2, 4, and 12 weeks of healing, respectively (Table 2). There were no statistically significant differences between the two groups at the same healing time ($P = .3103$ at week 2, $P = .4964$ at week 4, $P = .4919$ at week 12). In addition, no statistical difference in mean ISQ was observed for either the test group ($P = .9641$ for 2 weeks, $P = .4992$ for 4 weeks, $P = .4193$ for 12 weeks) or the control group ($P = .2091$ for 2 weeks, $P = .5224$ for 4 weeks, $P = .9369$ for 12 weeks) between week 0 (baseline) and any healing time. Changes in mean ISQ were further analyzed. The changes in ISQs from baseline (week 0) between the two groups showed no statistical differences ($P = .1619$ at week 2, $P = .5381$ at week 4, $P = .3049$ at week 12) (Fig 3).

Histologic Observations

The histopathologic assessment through microscopic observation revealed no differences between the test and control groups. In addition, there was no evidence of acute inflammation in any specimen examined. Minimal to mild chronic inflammation was indicative of the expected foreign-body response, and comparable levels of fibrosis were increased over time. More importantly, no evidence of bacterial infection was seen within the TM pores of any test group implants or on the threaded portion of the test or control group implants.

Representative histologic images of six and a half threads were taken at the coronal end, beginning at the second thread of each implant, for the control group, and corresponding images were taken within the same distance for the test group by including the Ta porous portion (Fig 4). Newly formed bone was first seen between threads in both groups and within the pores of the test implants at 2 weeks (Figs 4a and 4d). Subsequent bone remodeling was observed at 4 weeks, and

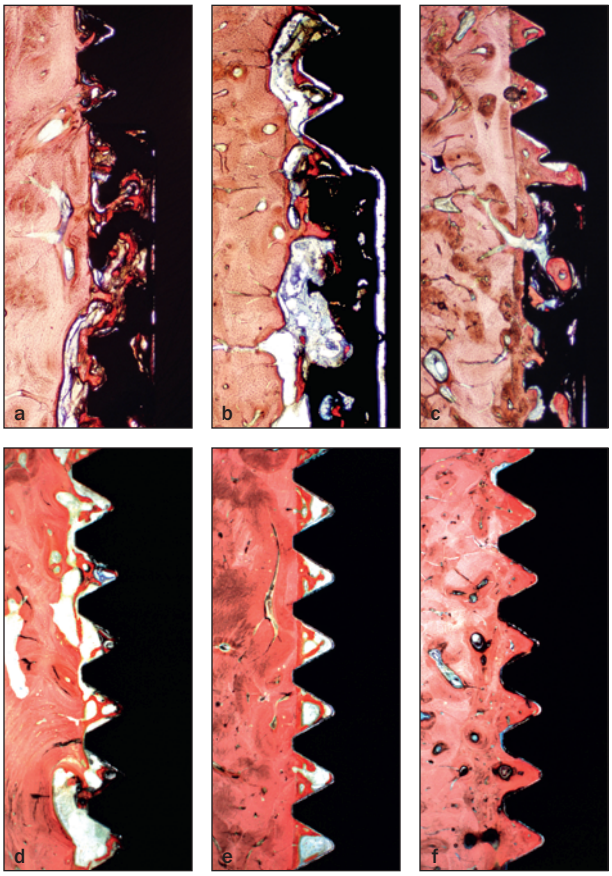

Fig 4 Representative histologic observations in *(top row)* test group and *(bottom row)* control group. In the test group, new bone formation within the implant pores as well as onto the threads was first seen at 2 weeks. Subsequently, bone remodeling took place during healing, similar to the threaded part of the implants in the control group (Sanderson and Van Gieson; original magnification ×2).

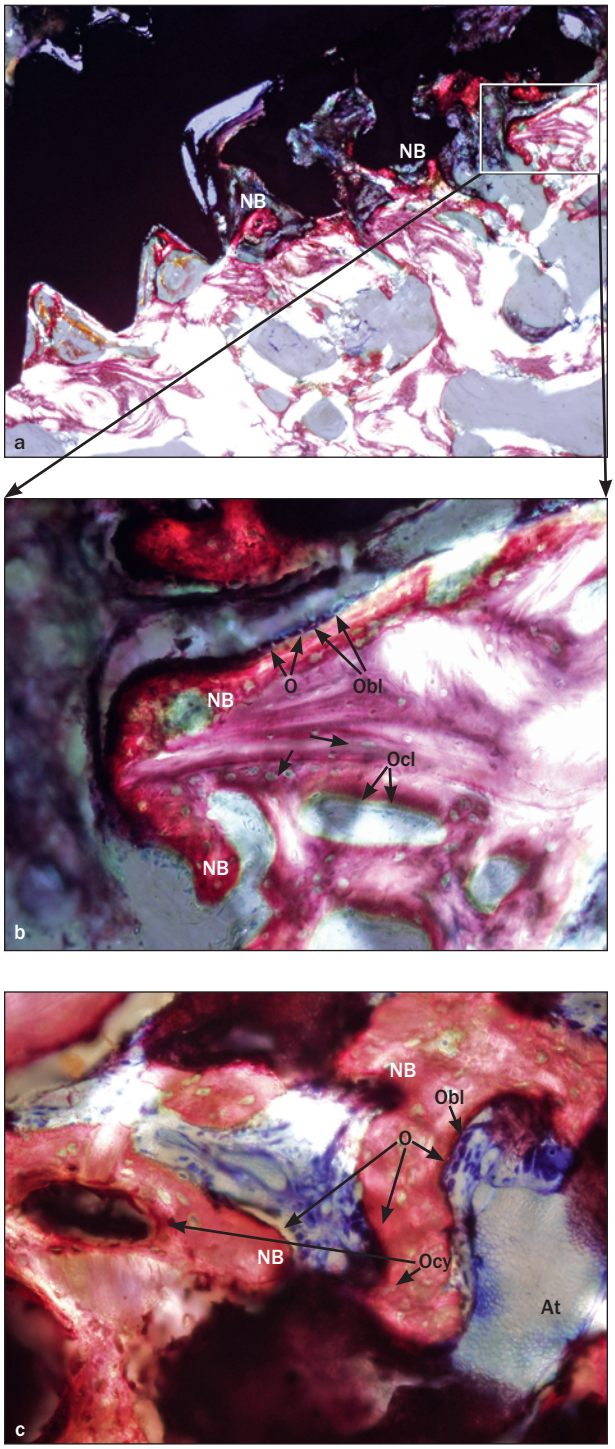

Fig 5 At 2 weeks after implantation, new bone (NB) was found in both *(a)* the threaded and *(b)* the porous regions in the test group (original magnifications ×4 and ×20, respectively). The NB was extensive at the Ta-based porous surface and *(c)* infiltrated into the interior surfaces of the porous region (original magnification ×40) (Sanderson and Van Gieson). At = adipose tissue; O = osteoid; Obl = osteoblast; Ocl = osteoclast; Ocy = osteocyte.

a thin layer of newly mineralized bone was observed on both the Ta strut surface and the titanium thread surface (Figs 4b and 4e). By week 12, newly formed trabecular bone appeared to be thicker, denser, and more abundant in the pores and between threads (Figs 4c and 4f) than the earlier time periods. Newly mineralized woven bone at various locations of a 2-week sample in the test group was confirmed at different magnifications (Fig 5). New bone was observed within the threaded region (Fig 5a), in direct apposition to the surfaces of Ta struts (Fig 5b), and within the internal porous region (Fig 5c). The presence of osteoblasts, osteoid, and osteoclasts

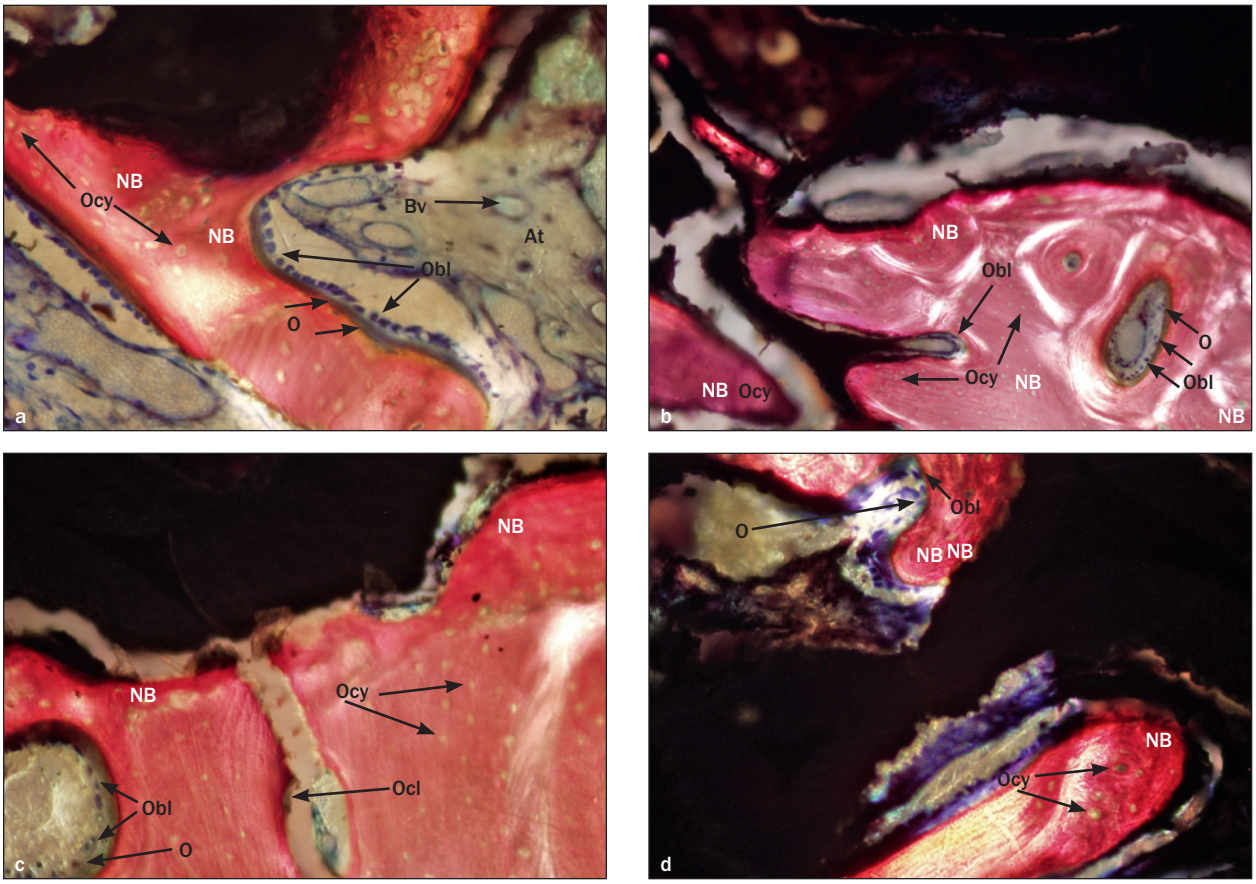

Fig 6 Progression of new bone formation in the test group at *(a and b)* weeks 4 and *(c and d)* 12 weeks. Adipose tissue (At), new bone (NB), osteoid (O), osteoblast (Obl), osteoclast (Ocl), blood vessels (Bv), and osteocytes (Ocy) were noted *(a and c)* at the Ta surface and *(b and d)* within the porous regions (Sanderson and Van Gieson; original magnification ×60).

indicated that bone apposition and remodeling were taking place during the early stage of immature woven bone formation. After 4 weeks of healing, it was evident in the test group that new bone apposition to the Ta strut surface was continuous (Fig 6a) and that new bone had formed in the deeper internal pores (Fig 6b). The new bone seen at 12 weeks appeared to be more mature trabecular bone, not only at the surface (Fig 6c) but also within the porous space (Fig 6d).

Histomorphometric Findings

The histomorphometric data at the interface and at the defined ROI are presented in Table 3. The %BIC with newly formed bone was not statistically significantly different at any time points between the test and control groups ($P = .9092$ at week 2, $P = .0557$ at week 4, $P = .3602$ at week 8). Also, both the test and control groups showed significantly higher %BIC at 12 weeks ($P < .0001$) than the corresponding %BIC values at 2 or 4 weeks, respectively. The %NBTA was not significantly different ($P = .2450$ at week 2, $P = .0964$ at week 4, $P = .8324$ at week 12) between the two groups at any given observation time, but both groups showed a higher %NBTA at 12 weeks ($P < .0001$) than at 2 or 4 weeks. Furthermore, %NBPA at 12 weeks was significantly higher than that at 2 or 4 weeks ($P < .0001$). A small amount of %OIC existed at each healing time for both groups. In the test group, %OPA showed a slight increase during healing. No statistical analysis was performed for either %OIC or %OPA.

Correlations

During the healing period from 2 weeks to 12 weeks, the individual %BIC values and %NBTA values did not show statistically significant correlations with corresponding ISQs (%BIC: Pearson correlation coefficient 0.285; %NBTA: Pearson correlation coefficient 0.035). Further, there was no statistical correlation between the individual %NBPA values and corresponding ISQs, insofar as newly formed bone inside the Ta pores was applicable to the test group only (%NBPA: Pearson correlation coefficient 0.167).

Table 3 Histomorphometric Data (n = 8)*

Parameter/group	Week 2	Week 4	Week 12	*P* value over healing
%BIC				
Test	33.74 ± 9.44	35.52 ± 4.86	63.98 ± 10.66	.7829, wk 2 vs wk 4 < .0001, wk 4 vs wk 12 < .0001, wk 2 vs wk 12
Control	33.15 ± 13.27	25.35 ± 8.68	73.13 ± 14.19	.2286, wk 2 vs wk 4 < .0001, wk 4 vs wk 12 < .0001, wk 2 vs wk 12
P at same time point	.9092	.0557	.3602	N/A
%OIC				
Test	0.35 ± 0.99	0.70 ± 1.17	0.43 ± 0.64	N/A
Control	0.58 ± 0.80	0.41 ± 0.63	0.05 ± 0.14	N/A
%NBTA				
Test	28.8 ± 9.88	32.43 ± 2.84	55.58 ± 10.73	.4636, wk 2 vs wk 4 < .0001, wk 4 vs wk 12 < .0001, wk 2 vs wk 12
Control	33.53 ± 8.62	25.61 ± 7.50	54.72 ± 8.36	.1149, wk 2 vs wk 4 < .0001, wk 4 vs wk 12 < .0001, wk 2 vs wk 12
P at same time point	.2450	.0964	.8324	N/A
%NBPA/test	14.24 ± 5.03	15.67 ± 5.84	36.63 ± 9.27	.7155, wk 2 vs wk 4 < .0001, wk 4 vs wk 12 < .0001, wk 2 vs wk 12
%OPA/test	2.81 ± 0.91	3.11 ± 1.77	3.57 ± 1.41	N/A

*Means ± standard deviations shown.

DISCUSSION

The present study was designed to investigate the effect of a newly developed Ta porous dental implant (test group) on bone ingrowth and stability during early healing in fresh extraction sockets in dogs. The test implants achieved similar outcomes to the control implants with respect to the degree of osseointegration and implant stability. In addition, the outcomes of the test implant in the present study were comparable to those previously reported for Ta porous implants placed in healed extraction sites in a canine model.[12] The significantly lower number of threads in the test implant and the presence of a Ta porous midsection in the test implants did not compromise mean ISQs (Table 2, Fig 3). Rather, the test implant achieved and maintained primary stability similar to that of the control implant. The average roughness of the microtextured surface of the control implant and the threaded portions of the test implants in this study has been reported to be 0.756 ± 0.073 μm.[24] The increase in apparent surface area of the test implant (unpublished manufacturer data), which resulted in comparable BIC and bone ingrowth, and the possibility of bone anchorage with the interconnected pores may have contributed to secondary stability during early healing. However, the contribution of the roughness of the Ta struts in the porous midsection has to be further investigated.

Other authors have found no significant correlations between ISQs and histomorphometric parameters.[25–27] In an experimental study in dog mandibles, no correlation was specified between ISQs and %BIC from measurements of eight different time points during a 3-month monitoring period.[26] Another study in dog mandibles found no correlation between ISQs and histologic data, such as BIC and peri-implant bone density, from the time of implant placement to retrieval at 1 and 3 months.[25] Further, Ito et al demonstrated no correlation between ISQs and %BIC after up to 4 weeks of assessment in the tibiae of minipigs.[27] In the present study, ISQ did not show any correlation with any histomorphometric parameters. However, the implications of ISQ measurements in initial stability and the progression of osseointegration during early stages of healing in both animal models and humans require further investigation.

The porous surface design examined here is not new to implant dentistry. A titanium beaded porous surface was applied to cylindric dental implant surfaces previously.[28] Deporter et al[28] tested implants with sintered bead surfaces placed in canine extraction sockets and reported that the percentage of bone ingrowth inside a sintered bead implant surface was 52% ± 16% at 4 weeks and exhibited no significant change (51% ± 16%) at 8 weeks. The present study showed that %NBPA ranged from 14% to 37% from 2 to 12 weeks. From the aspect of implant design, it

should be pointed out that there are several major differences between the test implant and the sintered bead implants that may affect stability and bone ingrowth. First, the stability of the current test implant was found to be comparable to the modern threaded design, whereas earlier unthreaded porous press-fit implant designs lacked external threads, which promote primary stability.[29,30] Second, the Ta porous biomaterial displayed an average pore size of 430 μm and up to 80% porosity,[13] while the pore size of sintered bead implants has been reported to range from 20 to 100 μm, with a mean porosity of 35%.[31] Third, the thickness of the porous Ta midsection is approximately 0.65 mm; in contrast, the sintered bead implants revealed a coalescence-like heterogenous shape, but no information is available regarding the thickness of the porous surface. Additional research with the test implant is suggested to evaluate the effects of bone ingrowth into Ta pores on secondary implant stability.

It has also been suggested that the optimal pore size for bone ingrowth is in the range of 100 to 500 μm and that interconnected porosity is critical to maintain vascularity, a prerequisite for continuing bone development inside porous biomaterials.[32] Interestingly, the 12-week values for %NBPA were significantly higher than at both earlier time points ($P < .0001$). A similar bone ingrowth phenomenon was reported in the canine femoral diaphysis model,[7] in which the amount of new bone observed within the Ta porous biomaterial increased from 13% at 2 weeks to 69% at 16 weeks. It is estimated that the bone formation into the Ta pores may be attributed to the physical properties of the osteoconductive Ta scaffold. Taken together, the exceptionally high porosity of the Ta porous biomaterial has been speculated to facilitate the migration of osteogenic and angiogenic cells deep into its inner pores, where they can proliferate, differentiate, and favorably compete with fibrous connective tissue.[13] Consequently, the histomorphometric data of the present study suggest that the tested implant is a promising alternative to currently available implants and should be further investigated. Although in the present study, the histopathologic assessment demonstrated that there were no infections with any of the test implants immediately placed into fresh extraction sites, the response of Ta porous dental implant to oral fluids, biofilm formation, and microbes remains to be clarified, as recently discussed by Bencharit et al.[13]

The present study has some potential limitations. First, different results might be obtained in a clinical setting. Second, the current study was limited to early healing periods up to 12 weeks. Further, the implants used in this study were not loaded, and there was no attempt to evaluate buccal and lingual healing dynamics around peri-implant sites. Further research is highly suggested to determine whether immediate loading of this Ta porous implant may affect the dynamics of bone ingrowth and increase implant stability during early healing.

CONCLUSION

In a canine immediate extraction socket model, both the test and control implants demonstrated comparable implant stability and percentage of bone-to-implant contact. In addition, bone ingrowth was evident within the tantalum porous section of the test implants during early healing.

ACKNOWLEDGMENTS

The coauthor Dr G. Romanos has not received any financial support from Zimmer Dental in connection with this study. The authors reported no conflicts of interest related to this study.

REFERENCES

1. Shimko DA, Shimko VF, Sander EA, Dickson KF, Nauman EA. Effect of porosity on the fluid flow characteristics and mechanical properties of tantalum scaffolds. J Biomed Mater Res B Appl Biomater 2005; 73:315–324.
2. Meneghini RM, Ford KS, McCollough CH, Hanssen AD, Lewallen DG. Bone remodeling around porous metal cementless acetabular components. J Arthroplasty 2010;25:741–747.
3. Levine B, Sporer S, Della Valle CJ, Jacobs JJ, Paprosky W. Porous tantalum in reconstructive surgery of the knee: A review. J Knee Surg 2007;20:185–194.
4. Stiehler M, Lind M, Mygind T, et al. Morphology, proliferation, and osteogenic differentiation of mesenchymal stem cells cultured on titanium, tantalum, and chromium surfaces. J Biomed Mater Res A 2008;86:448–458.
5. Levine B, Della Valle CJ, Jacobs JJ. Applications of porous tantalum in total hip arthroplasty. J Am Acad Orthop Surg 2006;14:646–655.
6. Levine BR, Sporer S, Poggie RA, Della Valle CJ, Jacobs JJ. Experimental and clinical performance of porous tantalum in orthopedic surgery. Biomaterials 2006;27:4671–4681.
7. Bobyn JD, Stackpool GJ, Hacking SA, Tanzer M, Krygier JJ. Characteristics of bone ingrowth and interface mechanics of a new porous tantalum biomaterial. J Bone Joint Surg Br 1999;81:907–914.
8. Bobyn JD, Poggie RA, Krygier JJ, et al. Clinical validation of a structural porous tantalum biomaterial for adult reconstruction. J Bone Joint Surg Am 2004;86-A(suppl 2):123–129.
9. Bobyn JD, Toh KK, Hacking SA, Tanzer M, Krygier JJ. Tissue response to porous tantalum acetabular cups: A canine model. J Arthroplasty 1999;14:347–354.
10. Wigfield C, Robertson J, Gill S, Nelson R. Clinical experience with porous tantalum cervical interbody implants in a prospective randomized controlled trial. Br J Neurosurg 2003;17:418–425.
11. Tsao AK, Roberson JR, Christie MJ, et al. Biomechanical and clinical evaluations of a porous tantalum implant for the treatment of early-stage osteonecrosis. J Bone Joint Surg Am 2005;87(suppl 2):22–27.
12. Unger AS, Lewis RJ, Gruen T. Evaluation of a porous tantalum uncemented acetabular cup in revision total hip arthroplasty: Clinical and radiological results of 60 hips. J Arthroplasty 2005;20:1002–1009.
13. Bencharit S, Byrd WC, Altarawneh S, et al. Development and applications of porous tantalum trabecular metal-enhanced titanium dental implants. Clin Implant Dent Relat Res 2013. [Epub ahead of print]

14. Kim DG, Huja SS, Tee BC, et al. Bone ingrowth and initial stability of titanium and porous tantalum dental implants: A pilot canine study. Implant Dent 2013;22:399–405.
15. Caneva M, Botticelli D, Morelli F, Cesaretti G, Beolchini M, Lang NP. Alveolar process preservation at implants installed immediately into extraction sockets using deproteinized bovine bone mineral—An experimental study in dogs. Clin Oral Implants Res 2012;23:789–796.
16. Covani U, Ricci M, Bozzolo G, Mangano F, Zini A, Barone A. Analysis of the pattern of the alveolar ridge remodelling following single tooth extraction. Clin Oral Implants Res 2011;22:820–825.
17. Chen ST, Darby IB, Reynolds EC. A prospective clinical study of non-submerged immediate implants: Clinical outcomes and esthetic results. Clin Oral Implants Res 2007;18:552–562.
18. Araujo MG, Linder E, Lindhe J. Bio-Oss collagen in the buccal gap at immediate implants: A 6-month study in the dog. Clin Oral Implants Res 2011;22:1–8.
19. Meredith N, Alleyne D, Cawley P. Quantitative determination of the stability of the implant-tissue interface using resonance frequency analysis. Clin Oral Implants Res 1996;7:261–267.
20. de Sanctis M, Vignoletti F, Discepoli N, Zucchelli G, Sanz M. Immediate implants at fresh extraction sockets: Bone healing in four different implant systems. J Clin Periodontol 2009;36:705–711.
21. Abed AM, Pestekan RH, Yaghini J, Razavi SM, Tavakoli M, Amjadi M. A comparison of two types of decalcified freeze-dried bone allograft in treatment of dehiscence defects around implants in dogs. Dent Res J 2011;8:132–137.
22. Becker W, Schenk R, Higuchi K, Lekholm U, Becker BE. Variations in bone regeneration adjacent to implants augmented with barrier membranes alone or with demineralized freeze-dried bone or autologous grafts: A study in dogs. Int J Oral Maxillofac Implants 1995;10:143–154.
23. Al-Hezaimi K, Iezzi G, Rudek I, et al. Histomorphometric analysis of bone regeneration using a dual-layer of membranes (dPTFE placed over collagen) in fresh extraction sites: In canine model. J Oral Implantol 2013 May 28. [Epub ahead of print]
24. Mazor Z, Cohen DK. Preliminary 3-dimensional surface texture measurement and early loading results with a microtextured implant surface. Int J Oral Maxillofac Implants 2003;18:729–738.
25. Schliephake H, Sewing A, Aref A. Resonance frequency measurements of implant stability in the dog mandible: Experimental comparison with histomorphometric data. Int J Oral Maxillofac Surg 2006;35:941–946.
26. Abrahamsson I, Linder E, Lang NP. Implant stability in relation to osseointegration: An experimental study in the Labrador dog. Clin Oral Implants Res 2009;20:313–318.
27. Ito Y, Sato D, Yoneda S, Ito D, Kondo H, Kasugai S. Relevance of resonance frequency analysis to evaluate dental implant stability: Simulation and histomorphometrical animal experiments. Clin Oral Implants Res 2008;19:9–14.
28. Deporter DA, Watson PA, Pilliar RM, et al. A histological assessment of the initial healing response adjacent to porous-surfaced, titanium alloy dental implants in dogs. J Dent Res 1986;65:1064–1070.
29. Szmukler-Moncler S, Salama H, Reingewirtz Y, Dubruille JH. Timing of loading and effect of micromotion on bone-dental implant interface: Review of experimental literature. J Biomed Mater Res 1998;43:192–203.
30. Elias CN, Rocha FA, Nascimento AL, Coelho PG. Influence of implant shape, surface morphology, surgical technique and bone quality on the primary stability of dental implants. J Mech Behav Biomed Mater 2012;16:169–180.
31. Cameron HU, Pilliar RM, Macnab I. The rate of bone ingrowth into porous metal. J Biomed Mater Res 1976;10:295–302.
32. Li JP, Li SH, Van Blitterswijk CA, de Groot K. A novel porous Ti6Al4V: Characterization and cell attachment. J Biomed Mater Res A 2005; 73:223–233.